Role for the fission yeast RecQ helicase in DNA repair in G2.

Article (Published Version)

Molecular and Cellular Biology

Role for the Fission Yeast RecQ Helicase in DNA Repair in G 2

Louise V. Laursen, Eleni Ampatzidou, Anni H. Andersen and Johanne M. Murray
***Mol. Cell. Biol.* 2003, 23(10):3692. DOI: 10.1128/MCB.23.10.3692-3705.2003.**

MOLECULAR AND CELLULAR BIOLOGY, May 2003, p. 3692–3705 Vol. 23, No. 10
0270-7306/03/$08.00+0 DOI: 10.1128/MCB.23.10.3692–3705.2003

Role for the Fission Yeast RecQ Helicase in DNA Repair in G_2

Louise V. Laursen,[1,2] Eleni Ampatzidou,[2] Anni H. Andersen,[1] and Johanne M. Murray[2]*

Department of Molecular Biology, Aarhus University, DK-8000 Aarhus C, Denmark,[1] and Genome Damage and Stability Centre, University of Sussex, Brighton BN1 9QG, United Kingdom[2]

Received 27 December 2002/Returned for modification 11 February 2003/Accepted 26 February 2003

Members of the RecQ helicase subfamily are mutated in several human genomic instability syndromes, such as Bloom, Werner, and Rothmund-Thomson syndromes. We show that Rqh1, the single *Schizosaccharomyces pombe* homologue, is a 3′-to-5′ helicase and exists with Top3 in a high-molecular-weight complex. *top3* deletion is inviable, and this is suppressed by concomitant loss of *rqh1* helicase activity or loss of recombination functions. This is consistent with RecQ helicases in other systems. By using epistasis analysis of the UV radiation sensitivity and by analyzing the kinetics of Rhp51 (Rad51 homologue), Rqh1, and Top3 focus formation in response to UV in synchronized cells, we identify the first evidence of a function for Rqh1 and Top3 in the repair of UV-induced DNA damage in G_2. Our data provide evidence that Rqh1 functions after Rad51 focus formation during DNA repair. We also identify a function for Rqh1 upstream of recombination in an Rhp18-dependent (Rad18 homologue) pathway. The model that these data allow us to propose helps to reconcile different interpretations of RecQ family helicase function that have arisen between work based on the *S. pombe* system and models based on studies of *Saccharomyces cerevisiae SGS1* suggesting that RecQ helicases act before Rad51.

The RecQ family of helicases is a subfamily of the DExH box containing DNA helicases. Homologues of the prototype bacterial RecQ helicases have been identified in a wide range of organisms spanning the prokaryotic kingdom up to humans. RecQ family helicases share extensive sequence homology within the seven helicase domains, but conservation in the remainder of the protein is generally limited to structural features such as acid-rich domains (10). Five RecQ family proteins have been identified in humans (37), and three syndromes represented by these proteins have been identified as defective in human genetic disorders: Bloom syndrome, Werner syndrome, and a subset of Rothmund-Thomson syndrome (RTS). Each syndrome presents with very different phenotypes: Bloom syndrome, which is associated with a defect in the BLM protein, is characterized by stunted growth, developmental problems, immunodeficiency, male infertility, and, at the cellular level, a slowing of S-phase progression and a dramatic increase in sister chromatid exchange and genomic instability (21). Werner syndrome, linked to a defect in the WRN protein, is a premature-ageing syndrome, and this is reflected at the cellular level by a decreased population-doubling potential (55). RTS (RECQ4 defective) comprises poikiloderma and growth deficiency, and RTS patients also exhibit aspects of premature ageing. All three syndromes are characterized by an increased predisposition to cancer, which is consistent with the increased chromosomal aberrations and hypermutability observed in cultured cells (31). These data suggest that each of these helicases contributes to maintaining genetic stability.

The prototype *Escherichia coli recQ* mutant is defective in the initiation of recombinational bypass of DNA damage during postreplication repair (PRR). PRR can be defined as the ability of the replication fork to reform and/or bypass unrepaired DNA damage by using recombination proteins. Purified *E. coli* RecQ helicase is capable of acting in concert with RecA during branch migration and drives the reaction in the direction opposite to that of RecBC, i.e., towards the original unrecombined substrates (24). In addition, when acting in conjunction with topoisomerase III (Top3), RecQ modifies the activity of Top3 in vitro to enable it to act as a type II topoisomerase, promoting plasmid catenation and/or decatenation (25). *E. coli* topoisomerase III, on its own, acts like a type I topoisomerase, changing the linking number of DNA in steps of one (16).

Both budding and fission yeasts have a single RecQ-like helicase. These are structurally most reminiscent of the human BLM protein. *Saccharomyces cerevisiae SGS1* was originally identified because its loss acted as a slow-growth suppressor of *top3* mutants. Subsequently, the Sgs1 protein was found to interact with Top3 and to act as a 3′-to-5′ helicase (3, 20). By use of the two-hybrid system, a potential interaction between Sgs1 and Top2 has also been demonstrated (49). In the fission yeast *Schizosaccharomyces pombe*, the RecQ homologue, Rqh1, was independently identified in screens for radiation-sensitive (*rad*) and hydroxyurea-sensitive (*hus*) mutants. Like *SGS1*, *rqh1* is not an essential gene and mutants lacking *rqh1* (*rqh1-d*) are significantly sensitive to DNA damage. *rqh1-d* mutants also display an increase in recombination when replication is inhibited (42, 45). Genetic analysis of the sensitivity of *S. pombe rqh1-d* mutants to UV-induced DNA damage defined a function for Rqh1 in the DNA "damage tolerance" pathway, which also requires recombination and checkpoint functions. This led to the suggestion that *rqh1* mutants are defective in the recombinational bypass of UV-induced DNA damage during the S phase (42).

The human BLM and the *S. cerevisiae* Sgs1 proteins have

* Corresponding author. Mailing address: Genome Damage and Stability Centre, University of Sussex, Falmer, Brighton BN1 9QG, United Kingdom. Phone: (44) 1273 877191. Fax: (44) 1273 678121. E-mail: j.m.murray@sussex.ac.uk.

been shown to be hexameric helicases (4, 28, 29), and both BLM and Sgs1 have been demonstrated to associate with Top3 directly (3, 20, 50), suggesting that complexes formed by this family of helicases are conserved through evolution. Because defects in RecQ family helicases affect recombination-dependent pathways in all systems studied, it is generally accepted that these proteins regulate recombination. We have investigated the genetic and biochemical interactions of *S. pombe* Rqh1 with Top3. Our data support a role for Rqh1 in recombination and lead us to propose a new role for Rqh1-Top3 in the repair of UV-induced DNA damage in G_2 cells via recombination-mediated repair.

MATERIALS AND METHODS

Genetics and cell biology techniques. Strains were constructed by using standard genetic techniques (38). The protocols for checkpoint measurements, cell scoring, and irradiation have previously been described (18). Indirect immunofluorescence microscopy was performed according to a protocol previously described (8). Briefly, cells were fixed in 3.7% (vol/vol) paraformaldehyde for 10 min and were stained with primary antibody (9E10 at 1:100, anti-Rqh1 antibody at 1:100, and anti-Rad51 and secondary antibody [fluorescein isothiocyanate-conjugated anti-mouse {Dako}] at 1:150). Synchronous cells were prepared by lactose gradients (2) or by elutriation of 4 liters of mid-log-phase cells (JE-5.0; Beckman Coulter).

PCR-based gene deletion and tagging. By use of a PCR-based method, the entire *top3* open reading frame (ORF) was replaced with either the *S. pombe* *ura4*$^+$ gene or the *S. cerevisiae* *LEU2*$^+$ gene (*top3-d*::*ura4*, *top3-d*::*LEU2*). A separate construct, where the *rqh1* helicase domain (bp 1527 to 2517, amino acids 526 to 869) was replaced by the *ura4*$^+$ gene (*rqh1-hd*:*ura4*), was also created. The *top3* and *rqh1* genes were tagged with sequences encoding either a C-terminal three-hemagglutinin (HA) or 13-MYC (MYC) epitope as previously described (1). Sequences encoding either an N-terminal 3×HA or N-terminal 2×MYC–six-His epitope were introduced at the N terminus of the ORF at the *top3* locus by first replacing the ATG with the *ura4*$^+$ gene and then by using fluoroorotic acid gene replacement to introduce the engineered fragment. The final construct, where the native promoter drives the tagged ORF, was checked by PCR and characterized by Western blot analysis.

Cloning of *top3* cDNA. Total RNA was prepared from *S. pombe* by using the Qiagen RNeasy minikit, and cDNA was produced with the Gibco BRL SuperScript II protocol. The *top3* cDNA was amplified by using PCR primers designed from the *top3*$^+$ sequence (Sanger Centre) and was cloned into pREP1 and pREP41HA vectors (15) behind a modified thiamine-repressible promoter (*nmt*), which fuses it to a sequence encoding three HA epitopes at the 5′ end. Overexpression of HA-Top3 resulted in a protein at a size corresponding to ≈78 kDa, consistent with the predicted molecular mass of 71.5 kDa for the untagged protein. The lethality of the *top3-d*::*ura4* strain could be complemented by ectopic expression of the cloned cDNA.

***rqh1* mutant alleles.** The *rqh1-K547A* and *rqh1-K547R* mutations were introduced into the cDNA by site-directed mutagenesis with the USE mutagenesis kit (Amersham Pharmacia). The *rqh1-r12* (*rqh1-T543I*) allele was PCR amplified from the genome, and the *Bam*HI-*Eco*NI fragment from this was used to replace 356 bp (1272 to 1628) of the *rqh1* ORF. The sequence of the cDNAs was confirmed by sequencing. To create genomic mutations of *rqh1-K547A* and *rqh1-K547R*, the cDNA was used to replace the *ura4* gene in *rqh1-hd*::*ura4* at the *rqh1* genomic locus. Correct integration was selected for by fluoroorotic acid resistance and was confirmed by PCR and Western blotting.

Helicase assays. The *rqh1* wild-type and mutant alleles were cloned (*Nde*I-*Sal*I) into pEPEX-HA and were in vitro translated by using the T7 quick-coupled TNT kit (Promega). Expression was checked by Western blot analysis. The in vitro translated proteins were then tested for their ability to release an [α-^{32}P]-labeled 40-mer oligonucleotide annealed to a single-stranded plasmid, M13mp18 (NEB). Some 40-mer (3.5 pmol) was hybridized to 3.5 pmol of plasmid by heating to 85°C and cooling slowly to room temperature. Two microliters of [α-^{32}P]dATP and 1.5 μl of Sequenase was added, the reaction materials were incubated at 30°C for 15 min, and the substrate was purified on a G-50 column. Helicase reactions (10 μl) containing 0.1 μl of labeled substrate (approximately 3.5 fmol) were performed in helicase buffer (25 mM Tris-HCl, pH 7.5, 1 mM dithiothreitol, 50 μg of bovine serum albumin/ml, 2 mM $MgCl_2$, and 2 mM ATP) for 30 min at 30°C. For each protein, three reactions were made containing increasing concentrations of in vitro translated protein: 2, 4, and 8 μl, the volume being made to a standard 8 μl with an "empty vector" in vitro translation mix. The reactions were stopped by the addition of 0.5% proteinase K, 100 mM Tris-HCl, pH 7.5, 200 mM EDTA, and 2.5% sodium dodecyl sulfate (SDS) and incubation at 37°C for 10 min. Products were analyzed by electrophoresis in a 15% nondenaturing polyacryamide gel and were subsequently autoradiographed.

Cell extracts, immunoprecipitation, and size fractionation. The protocols for total cell extracts, soluble extracts, size fractionation by using a Superdex 200 HR 10/30 (Pharmacia) column, and immunoprecipitation experiments have all been previously described (8). Soluble and/or insoluble fractionation was performed as previously described (12).

Antibodies. An *rqh1* N-terminal 1.085-kb fragment encoding amino acids 1 to 361 was PCR amplified by using primers incorporating *Nde*I and *Bam*HI sites and was cloned into pET16b (Novagen). The His-tagged protein, purified under denaturing conditions according to the manufacturer's instructions, was used for immunization of rabbits. The anti-Rqh1 antibody recognized a single band of approximately 175 kDa in trichloroacetic acid extracts of wild-type cells that was absent in *rqh1* null mutants and increased in size to ~190 kDa in the *rqh1-MYC* strain (Fig. 2f). The antibody was affinity purified against the antigen by using AminoLink Plus Coupling gel (Pierce). Rqh1-MYC or Top3-MYC was detected with anti-MYC monoclonal antibody (9E10; PharMingen), and Top3-HA was detected with anti-HA monoclonal antibody (Babco, Richmond, Calif.).

RESULTS

Rqh1 is a 3′-to-5′ helicase, and mutations in helicase domain 1 abolish helicase activity. The RecQ family has been demonstrated to have helicase activity in vitro. Since the Rqh1 helicase domains are highly conserved, we anticipated that Rqh1 would share this activity. To demonstrate this, we performed an in vitro helicase assay by using recombinant protein produced by coupled transcription-translation (Promega) in rabbit reticulocyte extract. When primed with either wild-type or mutant *rqh1* cDNAs, extracts were found to express a protein of the expected size (175 kDa) upon analysis by SDS-polyacrylamide gel electrophoresis (PAGE) (Fig. 1a). Extracts expressing wild-type Rqh1 were able to displace a radiolabeled 40-base oligonucleotide that had been previously annealed to single-stranded M13mp18 phage DNA (Fig. 1b). Extracts primed with empty vector were not active in this assay, demonstrating dependence on Rqh1. In a similar reaction, Rqh1 was also able to displace a 90-base oligonucleotide, although with lower activity (data not shown). We also demonstrated that, as expected, Rqh1 acts as a 3′-to-5′ helicase. In this experiment (Fig. 1c), an oligonucleotide (25 bases) was released from an 85-base oligonucleotide only when annealed to the 5′ end. An oligonucleotide (35 bases) annealed at the 3′ of the 85-base oligonucleotide was not a substrate for Rqh1-dependent displacement.

The original *rad12* mutant in the *rqh1* gene results in a T543I substitution in Rqh1 (42). *rqh1-T543I* mutant cells exhibit ionizing radiation (IR) and UV radiation sensitivities that are intermediate between those of wild-type cells and *rqh1-d* cells (Fig. 1d). The T543 residue is conserved in all RecQ family members and lies within the highly conserved 1a helicase domain, which contains the ATP binding site. To test if Rqh1-T543I is active as a helicase in vitro, we engineered the T543I mutation into the cDNA. Two further ATP binding site mutations, previously demonstrated in other systems to encode helicase-dead proteins, were also engineered as controls. The corresponding recombinant proteins were expressed in vitro by using the transcription-translation system (Fig. 1a). Neither the Rqh1-T543I mutant protein nor either of the two helicase-dead ATP site mutant control proteins (Rqh1-K547R and

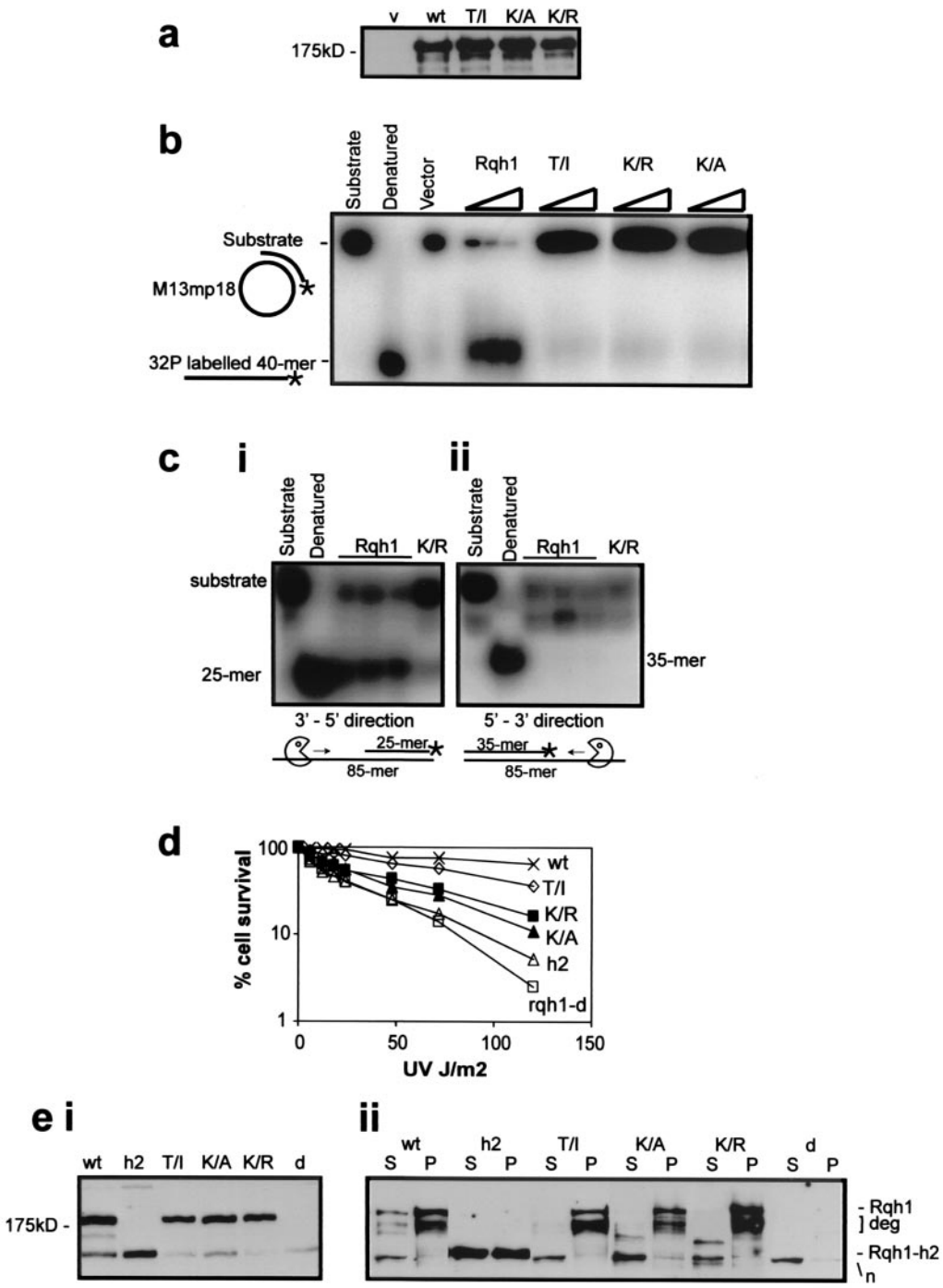

FIG. 1. Rqh1 acts as a helicase and mutations in helicase domain 1 abolish in vitro activity. (a) In vitro translation of Rqh1 alleles. Empty pEPEX-HA vector (v), vector containing wild-type *rqh1* (wt), or rqh1 mutants *rqh1-T543I* (T/I), *rqh1-K547A* (K/A), and *rqh1-K547R* (K/R) were used to prime TNT reticulocyte lysates, and proteins were identified following SDS-PAGE and Western blotting with anti-Rqh1 antibody. (b) Helicase assays. These were performed by using increasing amounts of primed lysates (as described for panel a above). The substrate, a 40-base ^{32}P-labeled oligonucleotide annealed to single-stranded M13, is shown diagrammatically to the left. Rqh1 has robust activity, while Rqh1-K547R (K/R), Rqh1-K547A (K/A), and Rqh1-T543I (T/I) have no activity. (c) Directionality of the Rqh1 helicase. Different primed lysates (as described for panel a above) were used. The substrate, an 85-base oligonucleotide annealed at each end to a ^{32}P-labeled 25-mer or 35-mer, is diagrammed below. Rqh1 displaced the 25-mer but not the 35-mer, showing it to have 3′-to-5′ helicase activity. Neither of the oligonucleotides was displaced by the helicase-dead protein Rqh1-K547R (K/R). (d) UV survival analysis of genomic mutants in *rqh1*. Symbols: ×, wild type; ■, *rqh1-K547R* (K/R); ▲, *rqh1-K547A* (K/A); ◇, *rqh1-T543I* (T/I); △, *rqh1-h2* (h2); and □, *rqh1-d.* (e) Western blots show the relative quantities of different Rqh1 proteins in total cell extracts (i) and their fractionation into soluble (S) and insoluble (P) extracts (ii). deg, degradation products, n, nonspecific band recognized by anti-Rqh1.

Rqh1-K547A) showed helicase activity in the in vitro assay (Fig. 1b).

Because the *rqh1-T543I* mutation leads to a phenotype that is less severe than that of the *rqh1-d* null mutant (42) we examined the phenotypes of the *rqh1-K547R* and *rqh1-K547A* ATP site helicase-dead mutants. Genomic mutants encoding these changes were created (see Materials and Methods). These mutants are at the *rqh1* locus and under the control of the native promoter. The response of both mutants to DNA-damaging agents (UV and ionizing radiation) and to inhibition of DNA synthesis (hydroxyurea) was compared to those of wild-type cells (*rqh1*$^+$) and of the *rqh1-T543I* strain. The two helicase-dead mutants are more sensitive than *rqh1-T543I*, approaching the *rqh1-d* null mutant in all assays (Fig. 1d and data not shown). This suggests that the helicase activity of Rqh1 is required for the majority of its biological functions, but the slight difference in survival compared to *rqh1-d* may reflect a function for Rqh1 that is independent of its helicase activity. Since *rqh1-T543I* is less sensitive, it is likely that *rqh1-T543I* is a hypomorphic mutant. However, it remains possible that Rqh1-T543I is helicase dead in vivo as well as in vitro. To investigate this further, we compared total protein level and distribution into soluble and insoluble fractions for Rqh1, Rqh1-T543I, Rqh1-K547R, and Rqh1-K547A proteins.

Cell extracts were prepared from log-phase cultures and fractionated into soluble and insoluble components as described in Materials and Methods. The insoluble fraction should contain the chromatin, along with membranes and organelles. Under the conditions used, Rqh1 was found to be largely insoluble, which would be consistent with Rqh1 being predominantly associated with chromatin or nuclear structures (Fig. 1e). The Rqh1-T543I, Rqh1-K547A, and Rqh1-K547R proteins were present at approximately wild-type levels (Fig. 1e, panel i), but virtually no soluble fraction was detected (Fig. 1e, panel ii). The Rqh1-h2 protein was found to partition equally between the soluble and insoluble fractions. The *rqh1-h2* (initially known as *hus2*) mutant causes a truncation in helicase domain 5 (Q789; stop codon) resulting in a null phenotype (Fig. 1d and reference 42). This increase in solubility is most likely to be due to the cytoplasmic localization of the mutant protein, which we observed by indirect immunofluorescence (data not shown).

Top3 is essential in the presence of an active Rqh1 helicase. Since RecQ family helicases interact both genetically and biochemically with Top3 in different model systems, we created a *top3* null allele (*top3-d*) by gene replacement in a diploid *S. pombe* strain (Fig. 2a). Consistent with the published data (22, 33), tetrad analysis demonstrated that *top3* is an essential gene in the presence of a wild-type *rqh1* gene but that, when *rqh1* is deleted, deletion of *top3* could be tolerated (Fig. 2b). It is generally considered that, in the absence of Top3, Rqh1 helicase activity processes an unknown DNA structure in a manner that causes lethality. Thus, consistent with the previously published data, we also observe that *top3-d* is tolerated in *rqh1-h2*, the helicase-dead mutants, *rqh1-K547R* and *rqh1-K547A*, and the hypomorphic *rqh1-T543I* mutant (Fig. 2b). Thus, our data are consistent with Top3 being required downstream of the Rqh1 helicase.

Because deletion of Top3 is lethal in the presence of an active helicase, we examined the consequences of overexpression of Top3. The *top3* cDNA was PCR amplified (see Materials and Methods) and was cloned into the expression vector pREP1. In addition, an active site mutant construct (Y330F in the conserved motif SYPTET) was created by site-directed mutagenesis. Overexpression of Top3 led to the phenotype of slightly elongated cells but had no effect on UV survival of wild-type cells (Fig. 2c and data not shown). However, overexpression of the active site mutant, Top3-Y330F, led to extensive cell death (Fig. 2c). The terminal phenotype was elongated cells with a range of defects, including fragmented nuclei, septa bisecting the nucleus (*cut* cells), and multiple septa (Fig. 2d). These data are consistent with the mutant protein interfering with the ability of the native protein to carry out its normal function (although it is still able to interact with Rqh1 [data not shown]). This dominant-negative phenotype was suppressed by deletion of *rqh1* (Fig. 2c). These data are again consistent with Top3 being required downstream of the Rqh1 helicase and the belief that, in the absence of Rqh1, a DNA structure that requires resolution by Top3 is not generated.

We next examined if loss of *top3* resulted in increased DNA damage sensitivity compared to that of the *rqh1-d* or *rqh1-T543I* single mutant. The double mutant *top3-d rqh1-d* showed no increase in sensitivity to UV or ionizing radiation when compared to *rqh1-d* (Fig. 2e), consistent with Top3 acting in the same pathway as Rqh1. However, the *top3-d rqh1-T543I* double-mutant sensitivity was intermediate between the sensitivities of *rqh1-T543I* and *rqh1-d* single mutants, suggesting that Top3 is required for the DNA damage response (Fig. 2e). However, analysis of the level of Rqh1-T543I protein in the *top3-d* background demonstrated that the protein level is significantly reduced when compared to a *top3*$^+$ background (Fig. 2f). Thus, the absence of Top3 appears to destabilize Rqh1-T543I, possibly because a direct protein association is disrupted or because the accumulation of suppressor mutations leads to a decrease in Rqh1 expression. A reduction in Rqh1-T543I protein level could account for the intermediate phenotype of the *rqh1-T543I top3-d* double mutant: if Rqh1-T543I is a partially functional protein (the result of a hypomorphic mutation), a reduced expression level might compromise the remaining function.

A physical interaction between Top3 and Rqh1. To examine the potential physical interaction between Rqh1 and Top3, we integrated sequences encoding 3×HA epitopes either 3′ or 5′of the ORF at the *top3* locus. Similarly, we integrated a 2×MYC–six-His encoding sequence 5′ of the ORF (see Materials and Methods). The *top3-HA* strain was slightly UV sensitive, but neither the *HA-top3* or *MYC–six-H–top3* strains showed any phenotype. In both cases, a single band could be detected by SDS-PAGE followed by Western blotting at a molecular weight consistent with the predicted size of Top3 plus the N-terminal tag (Fig. 3a). We performed reciprocal coimmunoprecipitation experiments for Rqh1 and HA-Top3. Immunoprecipitation with anti-Rqh1 antibodies coprecipitated the majority of HA-Top3 from *rqh1*$^+$ but not *rqh1-d* extracts (Fig. 3b). This indicates that Rqh1 and Top3 are present in the same complex in vivo. Likewise, immunoprecipitation with anti-HA coprecipitated Rqh1.

To further verify that Rqh1 and Top3 exist in a common complex, we fractionated cell extracts by using size exclusion

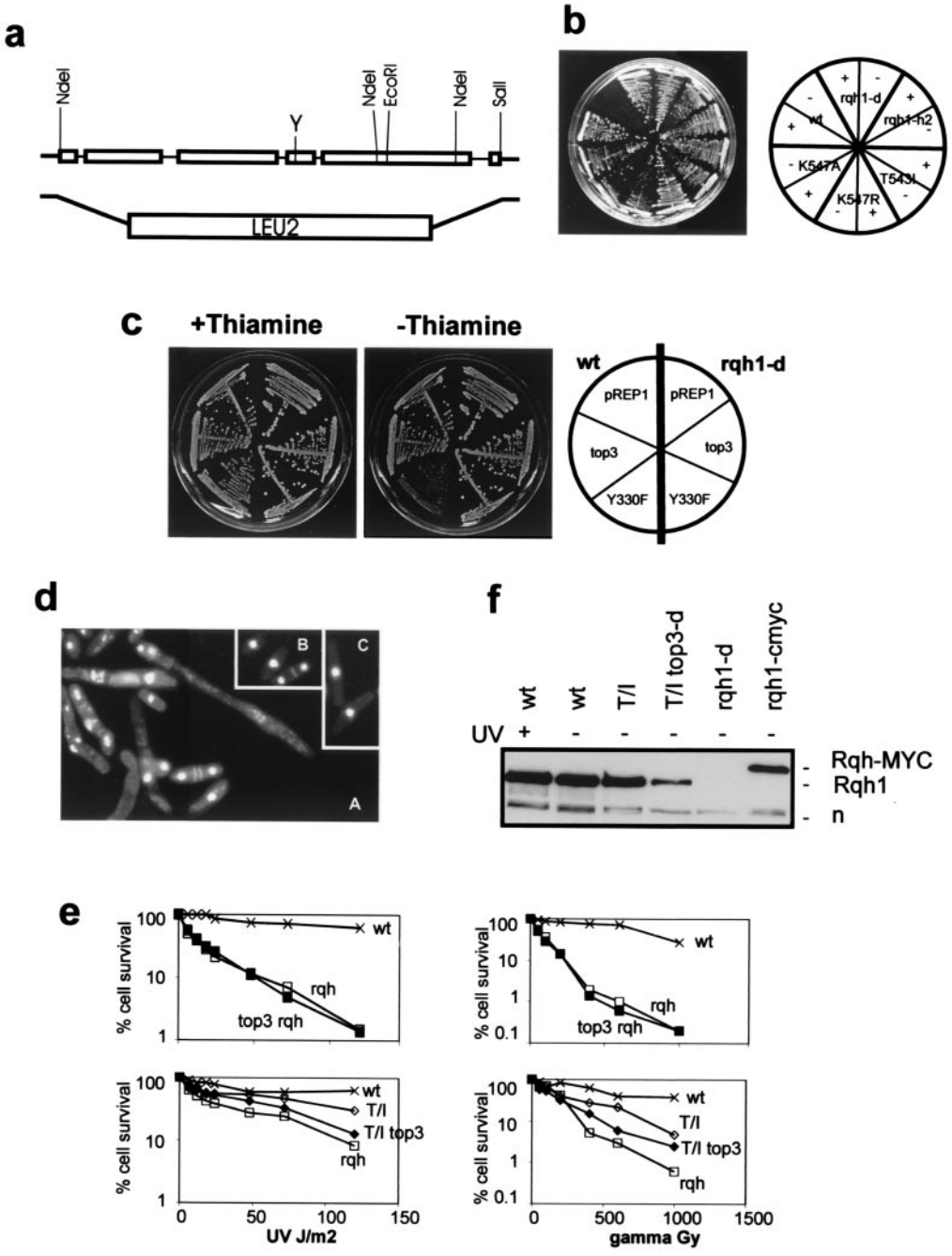

FIG. 2. Characterization of Top3. (a) Diagrammatic representation of the *top3* gene, showing the position of the exons and the active-site tyrosine 330 (Y) and the deletion strategy. (b) *top3-d* is viable in combination with *rqh1-d*, *rqh1-h2*, *rqh1-K547R*, *rqh1-K547R*, and *rqh1-T543I*. Cells, derived from tetrad analysis, were streaked to single colonies on rich media and were incubated for 3 days at 30°C. +, *top3*$^{+}$; −, *top3-d*; wt, wild type. (c) Overexpression of the Top3 active-site mutant, *top3-Y330F*, is lethal in wild-type cells but viable in *rqh1-d*. Cells were streaked to single colonies on minimal media with thiamine (+Thiamine) and were then replica plated to minimal media without thiamine (−Thiamine) to induce the expression of Top3-Y330F. (d) Wild-type cells overexpressing Top3-Y330F die elongated, with a range of defects, including degraded DNA, cuts, and multiple septa (inset A), compared to *rqh1-d* cells overexpressing the same construct (inset B) and wild-type cells overexpressing Top3, which are slightly elongated (inset C). (e) UV and IR sensitivity of *rqh1 top3* double mutants. Symbols: ×, wild type; □, *rqh1-d*; ■, *rqh1-d top3-d*; ◇, *rqh1-T543I*; and ◆, *rqh1-T543I top3-d.* (f) Western blot of total cell extracts showing Rqh1 protein levels in *top3*$^{+}$ and *top3-d* backgrounds. Rqh1 levels are decreased in the *top3-d* background (*rqh1-T543I top3-d* compared to *rqh1-T543I*). No change was observed in wild-type cells after UV irradiation (UV + wt). Log-phase cells were irradiated with 100 J/m^2 and allowed to recover for 1 h before total cell extracts were prepared by trichloroacetic acid precipitation. Rqh1-MYC migrates slightly higher than the native protein. n is a nonspecific band recognized by anti-Rqh1 shown as a loading control.

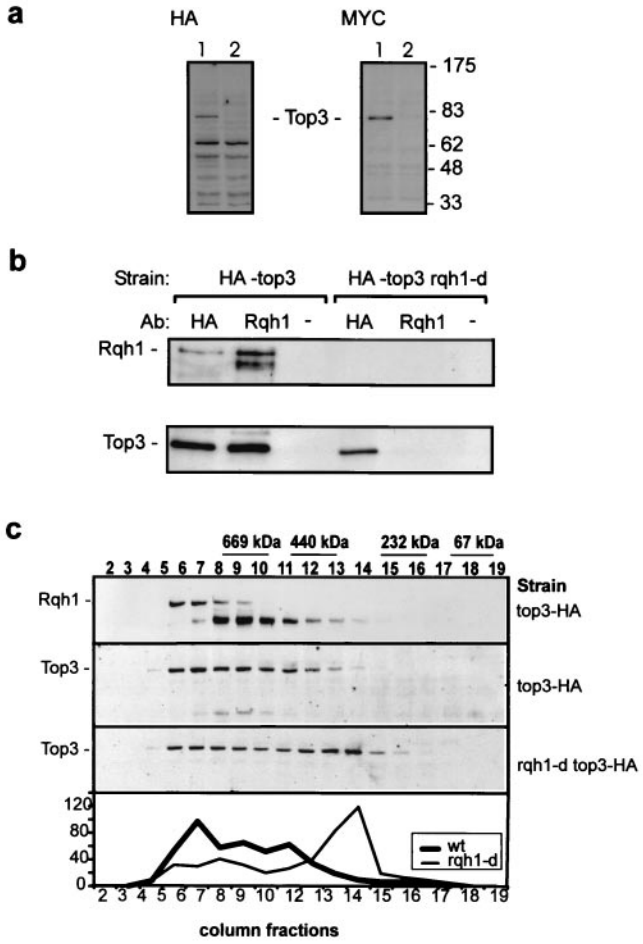

FIG. 3. Top3 and Rqh1 are associated in soluble cell extracts. (a) Western blot using 100 μg of total protein extract demonstrating the specificity of the anti-HA and anti-MYC antibodies to the N-terminally tagged Top3 proteins. Lanes: 1, *top3*-tagged strain; 2, equivalent untagged strain. Kilodaltons are given on right. (b) Reciprocal coimmunoprecipitation analysis of Rqh1 and HA-Top3. Two milligrams of total soluble extract was immunoprecipitated with an excess of either anti-HA or anti-Rqh1 antibody (Ab) from *HA-top3* or *HA-top3 rqh1-d* extracts and was analyzed by Western blotting by using anti-HA or anti-Rqh1 antibodies. (c) Size exclusion chromatography of soluble extracts from *top3-HA* (C-terminal HA tag) and *rqh1-d top3-HA* cells. Extract (1.5 mg) was loaded, and 10% of each fraction was analyzed for Rqh1 (anti-Rqh1 antibody) or Top3-HA (anti-HA antibody). Given is the relative intensity of Top3 band, which shows that in the absence of Rqh1 Top3-HA migrates in lower-molecular-weight fractions.

chromatography (Sephadex 200 column). Rqh1 was present in a complex of >700 kDa (Fig. 3c). The human BLM helicase has been found in a complex of similar size containing a hexamer of BLM molecules (29). Top3-HA was present in the same fractions as Rqh1, and when the experiment was repeated with *rqh1-d* extracts, a significant proportion of Top3-HA migrated in lower-molecular-weight fractions. This is consistent with disruption of an Rqh1-Top3 complex. Interestingly, Top3-HA did not run as a monomer in the absence of Rqh1, suggesting that it may form complexes with other proteins in addition to Rqh1. This is consistent with size fractionation of the *S. cerevisiae* Sgs1-Top3 complex (19).

Rqh1 acts with recombination proteins. During the unperturbed cell cycle, intrinsic DNA damage—most probably occurring during DNA replication—is processed by recombination proteins. The loss of recombination functions in *S. pombe* results in severe chromosomal instability and prolonged cell cycle delay (40). Presumably, during this delay, the aberrant DNA structures are repaired by alternative mechanisms. The Rqh1-dependent lethality of the *top3-d* mutation reflects the fact that Rqh1 activity creates lethal (or irreparable) DNA structures from this intrinsic DNA damage. We can thus use the lethality of *top3-d* as an assay to identify genetic backgrounds that do not generate the substrate that Rqh1 processes. In this way, we should be able to order the DNA-processing events that act on intrinsically produced aberrant DNA structures.

We first tested DNA integrity checkpoint mutants because it was previously found that *rqh1-d* caused synthetic lethality in *rad3-d* and *rad26-d* mutants but not in other checkpoint mutants (42). *top3-d* was not viable in *rad1-d*, *rad3-d*, and *rad26-d* mutants (Table 1). In addition, we tested *top3-d rqh1-d rad3-d* and *top3-d rqh1-d rad26-d* triple mutants for viability and found that neither was viable. These data indicate that the synthetic lethality previously observed between *rqh1-d* and *rad3-d* or *rad26-d* is not due to inappropriate regulation of Top3 activity. We have also previously demonstrated that Rqh1 acts with the Cds1 kinase in the same S-phase DNA damage tolerance response, which requires the recombination apparatus (42). *top3-d cds1-d* double mutants are inviable, indicating that Rqh1 is still able to act as a helicase in the absence of Cds1.

Recent work in *S. pombe* suggests that Rqh1 and Top3 function during the later stages of IR-induced double-strand break (DSB) repair by homologous recombination (9). If Rqh1 acts during recombination in unperturbed S phase, loss of recombination genes should prevent *top3-d* lethality because it would prevent the formation of the DNA structures that result in Rqh1-dependent *top3-d* inviability. We thus created double mutants between *top3-d* and a number of recombination mutants including *rhp51-d* (*recA*/*RAD51* homologue), *rhp54-d* (*RAD54* homologue), *rhp55-d* (*RAD51* paralogue), and *rad22-d* (*RAD52* homologue) (Table 1). Each of the four double mutants was viable but slow growing (Fig. 4a, panel i, left, and Table 1), indicating that Rqh1 indeed acts in recombination during normal cell growth.

The suppression of the *top3-d* lethality by loss of recombination genes is consistent with Rqh1 acting downstream of recombination in the processing of intrinsic DNA damage. In this scenario, which is consistent with the analysis of Top3 function in IR-induced DSB repair (9), loss of recombination genes prevents the formation of the DNA structures that result in Rqh1-dependent *top3-d* inviability. An alternative explanation of these data is that Rqh1 acts upstream of recombination proteins in the processing of intrinsic lesions. In this model, loss of $top3^+$ results in Rqh1 generating a lesion that becomes a substrate for an inappropriate and lethal attempt at recombination.

Overexpression of Top3 with an active-site tyrosine-to-phenylalanine mutation in $rqh1^+$ cells leads to cell death with highly elongated cells (Fig. 2c and d), similar to a terminal phenotype seen in spores germinated with a *top3* deletion (reference 22 and data not shown). Because this dominant-

TABLE 1. List of mutants[a]

Strain description	Viability
rqh1-d	+
rad3-d	+
rad3-d rqh1-d	−
rad3-d top3-d	−
rad3-d rqh1-d top3-d	−
rad26-d	+
rad26-d rqh1-d	−
rad26-d top3-d	−
rad26-d rqh1-d top3-d	−
rad1-d	+
rad1-d rqh1-d	+
rad1-d top3-d	−
rad1-d rqh1-d top3-d	+
cds1-d	+
cds1-d rqh1-d	+
cds1-d top3-d	−
cds1-d rqh1-d top3-d	+
rhp51-d	+
rhp51-d rqh1-d	+
rhp51-d top3-d	+
rhp51-d rqh1-d top3-d	+
rad22-d	+
rad22-d rqh1-d	−/+**
rad22-d top3-d	−/+*
rad22-d rqh1-d top3-d	+
rhp54-d	+
rhp54-d rqh1-d	+
rhp54-d top3-d	+
rhp54-d rqh1-d top3-d	+
rhp55-d	+
rhp55-d rqh1-d	+
rhp55-d top3-d	+
rhp55-d rqh1-d top3-d	+
rhp18-d	+
rhp18-d rqh1-d	+
rhp18-d top3-d	−
rhp18-d rqh1-d top3-d	+
uve1-d	+
uve1-d rqh1-d	+
uve1-d top3-d	−
uve1-d rqh1-d top3-d	+

[a] *, severe growth defect; **, most double mutants not viable; viable colonies have severe growth defect.

negative phenotype was suppressed in *rqh1-d* cells (Fig. 2c), we investigated whether it could also be suppressed by deletion of recombination proteins. In the recombination mutant strains *rhp51-d*, *rhp54-d*, *rhp55-d*, and *rad22-d*, overexpression of the active-site mutant was not lethal. This shows that the dominant-negative phenotype is suppressed by either deletion of *rqh1* or deletion of recombination genes (Fig. 4b) and that the suppression of lethality in the corresponding double mutants is not the result of a rapid accumulation of suppressor mutations.

UV sensitivity of *rqh1-d*, *top3-d*, and recombination mutants. We next looked at clonogenic survival following UV and ionizing radiation in the *rqh1-d*, *top3-d*, and recombination mutants. After ionizing radiation, like the previously characterized double mutants between *rqh1-d* and recombination gene deletions (42), double mutants between *top3-d* and recombination gene deletions and the triple *rqh1-d top3-d* recombination mutant were as sensitive as but not more sensitive than the single recombination mutant (Fig. 4c and data not shown). However, in response to UV irradiation, the sensitivity of *rqh1-d* and *rqh1-d top3-d* double mutants was rescued by concomitant loss of *rhp51* or *rhp55* (Fig. 4a, panels i and ii). Concomitant loss of *rhp54* did not result in an obvious rescue. Concomitant loss of *rad22* did rescue the UV sensitivity of *rqh1-d top3-d*, but the double *rad22-d rqh1-d* and *rad22-d top3-d* mutants have a severe growth defect, which makes the epistasis analysis difficult to interpret.

These data support the model in which Rqh1 and Top3 act within the recombination response to UV-induced DNA damage. UV survival of cells lacking Rqh1 and Top3 functions is increased in the absence of recombination. This suggests that, in the absence of recombination, DNA damage is not processed into a form that requires processing by Rqh1 and Top3. If the original damage is not a substrate for recombination (i.e., in *rhp51-d* or *rhp55-d* mutants), it can be repaired by an alternative pathway. If it is a substrate of recombination (i.e., *rhp*$^+$ strains) the damage is processed and a DNA structure is formed that must either be processed by Rqh1-Top3 or result in cell death. Interestingly, this could possibly explain the lack of rescue by *rhp54-d*: Rhp54 is thought to act later in recombination, whereas Rhp55 and Rhp51 are thought to act to initiate recombination. Once recombination is initiated, loss of a later step (i.e., *rhp54-d*) would not be expected to rescue the UV sensitivity because an alternative pathway is no longer possible.

Rqh1 and Top3 have been implicated in recombination repair of IR-induced DSBs in G_2 (9). To ascertain if there is a role for Rqh1 in the repair of G_2-induced UV damage and to verify the restoration of UV resistance by concomitant deletion of recombination genes, we treated G_2-synchronized wild-type, *rqh1-d*, *rhp51-d*, and *rqh1-d rhp51-d* cells with UV and assayed survival. *rqh1-d* cells are sensitive to low doses of UV in G_2, and this sensitivity is reversed by concomitant loss of *rhp51*. This provides evidence of a role of Rqh1 in G_2 repair of UV-induced DNA damage by recombination and confirms the rescue of *rqh1-d* sensitivity by loss of *rhp51* in a discrete cell cycle compartment.

Rqh1 and Top3 form foci following UV irradiation in G_2. The genetic evidence presented above indicates that Rqh1 and Top3 function in recombination after the Rhp51-dependent initiation step. This prompted us to search for further independent supporting evidence by examining protein localization before and after UV-induced DNA damage: first, we synchronized wild-type cells by centrifugal elutriation and examined the localization of Rqh1. Rqh1 localized to the nucleus throughout the cell cycle. During the majority of the cell cycle, Rqh1-dependent fluorescence overlapped with the DNA but was predominantly nucleolar. However, during and immediately after mitosis nuclei appeared diffusely stained and fluorescence was clearly present in areas of the nucleus that did not contain 4′,6′-diamidino-2-phenylindole (DAPI)-staining material (Fig. 5a).

Next, we examined Rqh1, MYC–six-His–Top3, and Rhp51

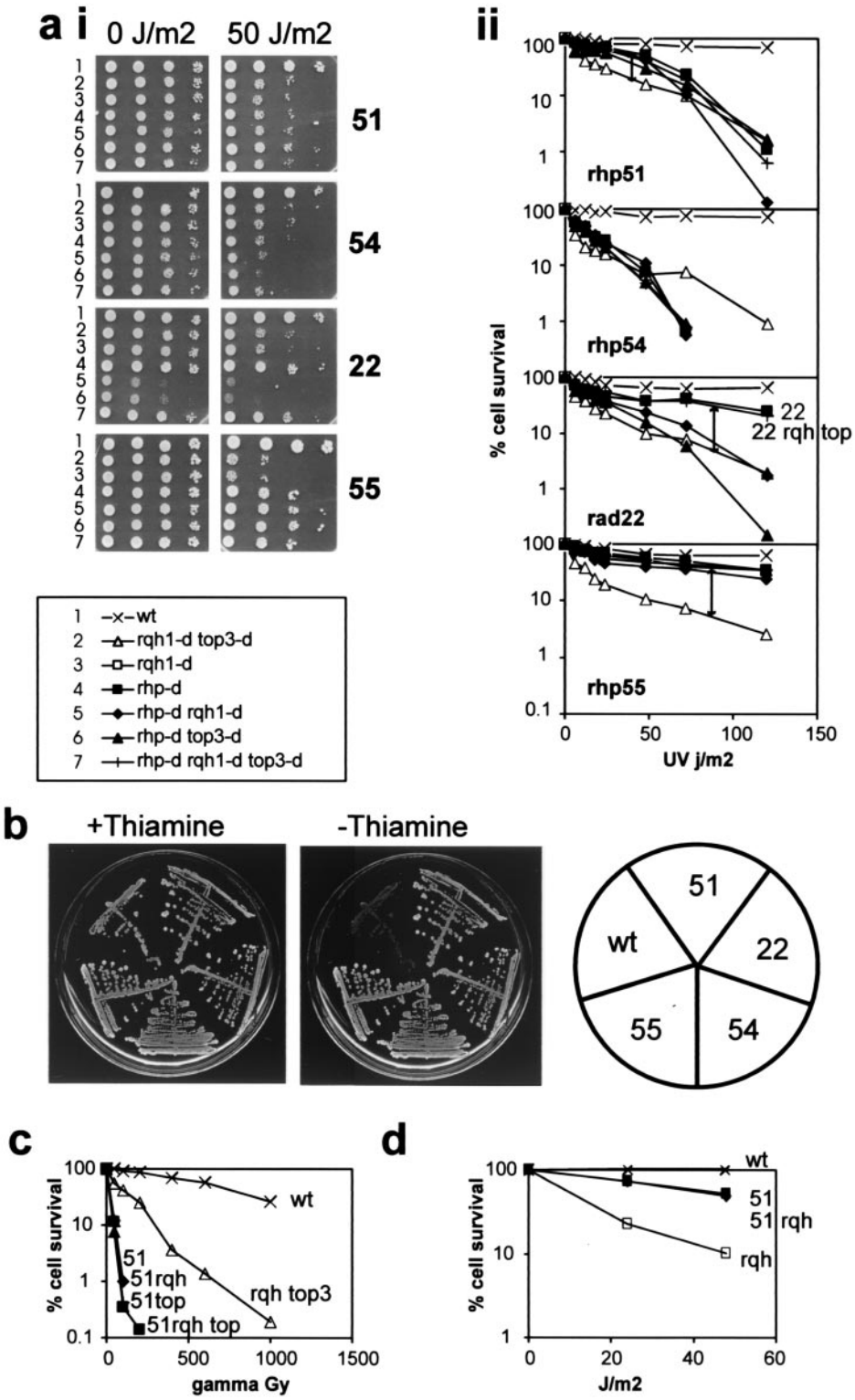

FIG. 4. *top3-d* mutants are viable in recombination mutant backgrounds. (a) Panel i, spot assays to show UV survival of recombination mutants *rhp51-d*, *rhp54-d*, *rad22A-d*, and *rhp55-d* with *rqh1-d* and *top3-d*. Strains are spotted in the order of the key. Panel ii, UV survival of recombination mutants *rhp51-d*, *rhp54-d*, *rad22A-d*, and *rhp55-d* with *rqh1-d* and *top3-d*. ↕ indicates that the suppression of the UV sensitivity of *rqh1-d top3-d* is seen by concomitant deletion of *rhp51*, *rhp55*, and *rad22* (only the triple mutant). (b) Top3-Y330F overexpression is viable in combination with *rhp51-d*, *rhp54-d*, *rhp55-d*, and *rad22-d*. Cells were streaked to single colonies on minimal media with thiamine (+Thiamine) and were then replica plated to minimal media without thiamine (−Thiamine) to induce the expression of Top3-Y330F. (c) IR survival of *rhp51-d*, *rqh1-d*, and *top3* mutants. (d) UV survival of wild-type and *rhp51-d*, *rqh1-d*, and *rhp51-d rqh1-d* mutants in G_2, showing that *rhp51-d* rescues the UV sensitivity of *rqh1-d* in G_2. Survival curves for the triple mutant lie under those for the single recombination mutant and thus are obscure in most panels.

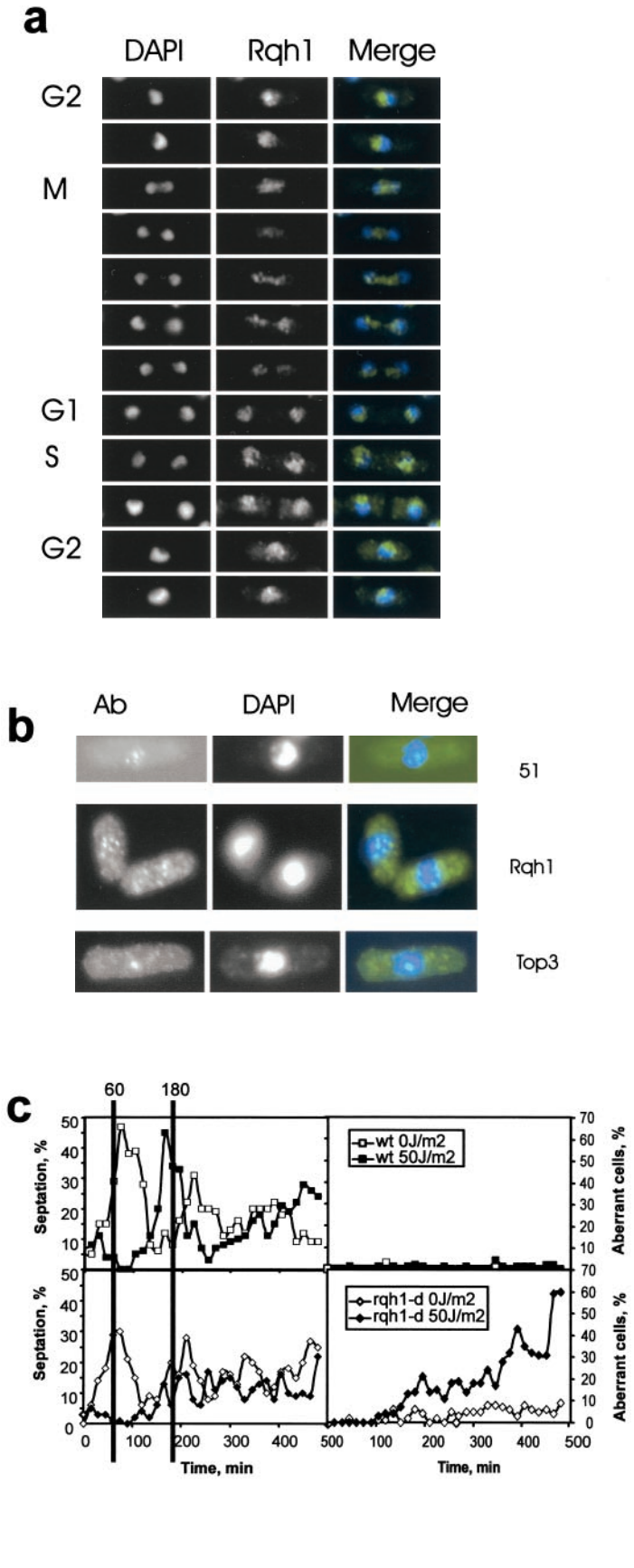

localization following treatment of cells with UV. After irradiation with 100 J of UV light/m^2, a significant proportion of cells exhibited distinct foci of Rqh1 in the DAPI-staining area of the nucleus (data not shown). In contrast, Rhp51 and MYC–six-His–Top3 were not detectable in unirradiated cells, but foci were observed following after UV irradiation (data not shown). To determine if the formation of these foci required passage through S phase, we first synchronized cells in G_2 and then irradiated with 100 J of UV light/m^2. By quantifying Rhp51, Rqh1, and MYC–six-His–Top3 foci, we observed an accumulation of foci following UV treatment of G_2 cells (Fig. 5b and d).

Treating G_2-synchronized cells with UV light leads to cell cycle arrest because of activation of the DNA damage checkpoints; thus, these cells remain in G_2 for some time before proceeding into mitosis. In order to determine whether the G_2 checkpoint was intact in *rqh1-d* cells, wild-type and *rqh1-d* cells were synchronized in G_2 by lactose gradients and were irradiated with 100 J of UV light/m^2. Both strains delayed mitosis for ~90 min at 29°C following irradiation, indicating an intact G_2-M checkpoint (Fig. 5c, left), but the *rqh1-d* strain lost viability, which correlated with the accumulation of aberrant postmitosis structures as the cells proceeded through mitosis (Fig. 5c, right).

A comparison of the temporal kinetics of Rqh1 and MYC–six-His–Top3 focus formation with the formation of Rhp51 foci (Fig. 5d) and comparison with the progression of the cells into mitosis (Fig. 5c) proved to be informative: Rqh1 foci are observed more rapidly than are Rhp51 foci (10 min after irradiation). However, the number of cells with foci increases more slowly than the number of cells exhibiting Rhp51 foci. Rhp51 foci are maximal approximately 1 h following treatment. At this point, the proportion of cells with Rqh1 foci is still increasing. There are fewer cells with MYC–six-H–Top3 foci, and fewer MYC–six-H–Top3 foci per cell (this may be an artifact of the detection), and these appear in elongated G_2 cells at later times. By the 180-min time point >50% of cells have undergone mitosis, but only elongated G_2 cells with a single nucleus (i.e., arrested, premitotic cells) were scored.

Several interesting observations arise from this analysis: we see that, in the absence of *rqh1*, no MYC–six-H–Top3 foci accumulate, indicating (as expected from the biochemistry) that Top3 foci are totally dependent on Rqh1. However, Rhp51 foci still appear in the absence of *rqh1* but with altered kinetics (Fig. 5d). In *rqh1-d* cells, Rhp51 foci are increased in the absence of irradiation (unirradiated and 10-min time points) and following irradiation the proportion of cells with Rhp51 foci increases more slowly. However, by 180 min the numbers are similar to those for *rqh1*$^+$ cells. Since *rqh1-d* cells and *rqh1*$^+$ cells enter mitosis with approximately the same kinetics following irradiation, while *rqh1-d* cells accumulate gross postmitotic aberrations (Fig. 5c), this suggests that recombination intermediates form but may not have been correctly processed or resolved. Again, this would be consistent with recombination occurring upstream of Rqh1 and Top3.

If the formation of Rqh1 and Top3 foci was always dependent on the initiation of recombination, we would anticipate that Rqh1 and MYC–six-H–Top3 foci would not form in *rhp51-d* mutant cells in G_2. However, both Rqh1 and MYC–six-H–Top3 foci are seen in *rhp51-d* cells following UV irradiation (Fig. 5d). The Rqh1 foci were slightly reduced, but the MYC–six-H–Top3 foci are increased. In order to understand and possibly reconcile these observations, we examined the UV response pathways in which Rqh1 and Rhp51 might act. Fission yeast contains two separate excision repair pathways that act to remove UV-induced DNA damage: the canonical nucleotide excision repair (NER) pathway and the UVDE pathway (54). The UVDE pathway is restricted to *S. pombe*, some bacteria, and several other eukaryotic microorganisms. In *S. pombe* it is known that the Uve1 enzyme nicks DNA immediately 5′ of the DNA lesion (30). Following this, the nick is processed by one of two separate pathways, which involve the FEN1 homologue Rad2 and the recombination machinery (53). In addition to the physical removal of UV-induced DNA damage, mechanisms exist to bypass the lesions by translesion synthesis or recombination. These are known as damage tolerance or PRR mechanisms. In the budding yeast *S. cerevisiae*, PRR depends on *RAD6*, encoding an E2 ubiquitin-conjugating enzyme, and *RAD18*, encoding a RING finger protein (6). It has been previously demonstrated that the fission yeast homologue of Rad18, Rhp18, is required for the survival of UV damage in G_2 (48).

If Rqh1 and Top3 are acting in a recombination repair pathway following UV-induced DNA damage in G_2, it is likely to be part of the Uve1-dependent repair process or the damage tolerance (PRR) pathway. In the absence of the UVDE pathway (*uve1-d* mutant), UV-induced DNA damage is repaired by the NER pathway, which is not expected to involve recombination. Indeed, we find that, in *uve1-d* mutants, Rhp51 foci are reduced following irradiation of G_2 cells (Fig. 5e). (In this analysis cells were only scored up to 60 min postirradiation to ensure that the results were not biased by erroneously scoring

FIG. 5. Immunolocalization of Rqh1 and formation of Rhp51, Rqh1, and Top3 foci. (a) Immunolocalization of Rqh1 through the cell cycle. Representative cells are shown. Rqh1 was visualized by using anti-Rqh1 antibody at 20-min intervals as a synchronous population of wild-type cells proceeded through the cell cycle. Cells were counterstained with DAPI to visualize the nucleus. In postmitotic G_1 cells, Rqh1-dependent fluorescence is seen in regions of the nucleus that do not stain with DAPI. (b) Rhp51, Rqh1, and Top3 foci in *MYC–six-H–top3* cells synchronized in G_2 by centrifugal elutriation and irradiated with 100 J of UV light/m^2. Commercial human anti-RAD51 antibody (Santa Cruz H-92) was used to visualize Rhp51, anti-Rqh1 was used to visualize Rqh1, and anti-MYC (PharMingen 9E10) was used to visualize Top3. (c) The G_2 checkpoint delay and entry into mitosis of wild-type and *rqh1-d* cells after UV. G_2 cells were prepared by lactose gradients and were irradiated with 100 J of UV-C light/m^2. Mitotic progression, as scored by septation analysis, and the percentage of aberrant mitoses were scored at 15-min intervals following methanol fixation and subsequent DAPI and Calcofluor staining. (d) Kinetic analysis of Rhp51, Rqh1, and Top3 focus formation in *MYC–six-H–top3*, *MYC–six-H–top3 rhp51-d*, and *MYC–six-H–top3 rqh1-d* cells synchronized in G_2 and irradiated with 100 J of UV light/m^2. (e) Rqh1 and Rhp51 focus formation in the indicated mutant strains synchronized in G_2 and treated with 100 J of UV light/m^2. Genotypes and percentage of cells showing foci are shown. (f) UV survival of *rhp51-d* and *uve1-d* to show that the double mutant is more sensitive than either single mutant. Symbols: ×, wild type; ■, *rhp51-d*; ◇, *uve1-d*; and ●, *rhp51-d uve1-d*.

cells passing through mitosis into the following S phase). However, Rqh1 foci were not decreased, indicating that these can be formed independently of Uve1 and Rhp51.

We next looked at the role of the Rhp18-dependent pathway and found that Rhp51 foci were decreased in *rhp18-d* mutant cells following irradiation. This suggests that both the *uve1*-dependent and the *rhp18*-dependent pathways contribute to Rhp51 focus formation (Fig. 5e). Unexpectedly, however, following irradiation of a *rhp18-d uve1-d* double mutant, Rhp51 foci were increased compared to the foci of the respective single mutants (Fig. 5e). One possible explanation of this would be that loss of both pathways results in a deregulation of repair that leads to the accumulation of DSBs, which activates alternative recombination pathways for repair. Indeed, when we analyzed the other double mutant, *uve1-d rqh1-d*, we also saw an increase in Rhp51 foci compared to foci of each single mutant (Fig. 5e). Thus, while we can draw some conclusions from these data, it is not possible to use the appearance of Rhp51 foci to define the pathways in which Rqh1 is involved.

Rqh1 foci, like Rhp51 foci, were significantly decreased in an *rhp18-d* mutant following UV irradiation (Fig. 5e). This suggests that Rqh1 is required for Rhp18-dependent processes in G_2. However, in the *uve1-d rhp18-d* double mutant, Rqh1 foci were reduced following irradiation. This is in contrast to the increase seen for Rhp51 foci. This suggests that the increased Rhp51 foci are independent of Rqh1. Since Rqh1 foci were also moderately decreased in the *rhp51-d* strain, we examined Rqh1 focus formation in an *rhp18-d rhp51-d* double mutant. In this case Rqh1 foci were also reduced following irradiation (Fig. 5e). Thus, Rqh1 foci result from Rqh1 functions that are downstream of both Rhp18 and Rhp51. This leads us to propose a model where Rqh1 and Top3 are required both upstream and downstream of Rhp51-dependent recombination (Fig. 6): Rqh1 and Top3 are required downstream of Rhp18 in an Rhp18-dependent pathway and are also required downstream of Rhp51. Since *rqh1* and *rhp51* are epistatic to each other, while neither is epistatic to *rhp18* or *uve1* (Fig. 5f and references 42 and 48), we have to propose that both Rqh1 and Rhp51 are required for the recombination-dependent subpathways of Rhp18-dependent repair and Uve1-dependent excision repair. This leads to the prediction that Rqh1 acts upstream of Rhp51 in the Rhp18-dependent pathway, since, if it were acting solely downstream of Rhp51, a deletion of *rhp51* would abolish Rqh1 focus formation. This is consistent with the observed increase in MYC–six-H–Top3 foci in an *rhp51-d* strain, as they would no longer be removed by recombination in the Rhp18 pathway.

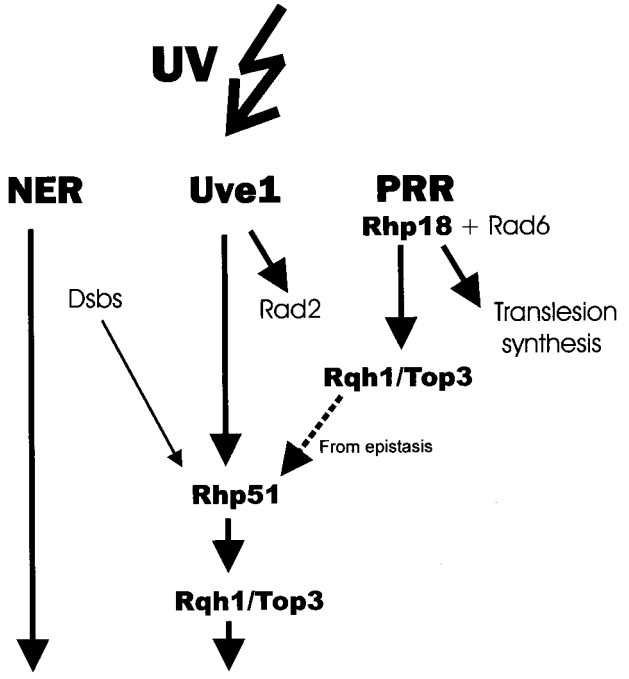

FIG. 6. Model of the roles of Rqh1 and Top3 in the repair of UV damage. In *S. pombe* UV damage is repaired by the classic NER and UVDE pathways. Damage can also be bypassed by translesion synthesis and recombination in PRR pathways mediated by Rhp6 and Rhp18 (homologues of budding yeast Rad6 and Rad18 proteins). Rhp51 has been reported to act in the recombination subpathway of UVDE (35) but is not epistatic to *uve1* (Fig. 5f), which is consistent with it also having a role in recombinational bypass in PRR, as has been shown for Rad51 (6). Rhp51 is also required for the repair of DSBs that can occur by a variety of means, including the repair of UV lesions on opposing strands (thin arrow). Rhp51 foci are reduced in either *uve1-d* or *rhp18-d*, supporting its roles in the UVDE and Rhp18-dependent pathways. Rqh1 foci are dependent on Rhp18 and Rhp51; therefore, Rqh1 is downstream of Rhp18 in PRR and downstream of Rhp51. The requirement for Rhp51 downstream of Rqh1 in PRR (dashed line) is based on epistasis, since *rqh1* and *rhp51* are epistatic to each other while neither is epistatic to *uve1* or *rhp18*.

DISCUSSION

Two conclusions arise from our analysis of Rqh1 and Top3: (i) using genetics and cell biology, we provide evidence that Rqh1 and Top3 function downstream of Rhp51-mediated strand invasion and downstream of an Rhp18-dependent pathway in response to UV-induced DNA damage in G_2, and (ii) we identify a role for Rqh1 and, by association, Top3 in the repair of UV damage during G_2.

Previously published data, discussed below, are consistent with, and strengthened by, our ordering of Rqh1-Top3 and Rhp51 functions during recombination. Our identification of a role for Rqh1-Top3 function during the response to UV-induced damage in G_2, which is additional to the previously demonstrated role in DNA damage tolerance, PRR during S phase, and IR-induced DSBs, extends the range of processes in which RecQ family helicases are involved.

Characterization of Rqh1 and Top3 in *S. pombe*. The function of RecQ family helicases is always closely linked to Top3 and associated with recombination (26, 52). However, it remains unclear where RecQ helicases act during these complex processes. In recent years, a role for recombination in processing aberrant DNA structures that arise either spontaneously or at sites of DNA damage during DNA replication has become apparent (14, 34, 36). In *E. coli*, RecQ functions in a RecF-dependent process that allows the recovery of DNA replication following DNA damage. This is proposed to involve the processing of nascent DNA at blocked replication forks prior to the resumption of DNA synthesis (13). In the absence of RecQ, *E. coli* cells become hyperrecombinogenic, a result of the persistence of recombinogenic DNA ends. A similar role

for eukaryotic RecQ helicases in the restoration of replication forks has been proposed (27).

Both *S. pombe* and *S. cerevisiae* have a single RecQ-related helicase, Rqh1 and Sgs1, respectively. *S. pombe rqh1-d* mutant cells are highly DNA damage sensitive. In part, this results from an inability to tolerate DNA damage in S phase (42). This is consistent with the bacterial model and also with the observation that Rqh1 loss results in elevated spontaneous and induced recombination (17, 45). The relatively dramatic DNA damage sensitivity of *rqh1-d* mutants (when compared to *S. cerevisiae sgs1* null mutants) makes *S. pombe* an attractive organism for the study of eukaryotic RecQ helicases. A further advantage of *S. pombe* is the fact that rapidly growing cells spend the majority of the cell cycle in G_2, making analysis of DNA damage response in this part of the cell cycle relatively simple. To further characterize Rqh1 function, we deleted the *top3* gene. *top3* is essential in the presence of *rqh1*$^+$ but becomes inessential when *rqh1* is deleted. This observation, which is consistent with reports from other groups (22, 33) published while this work was ongoing, allows access to a simple assay: we reasoned that mutants in which *top3* deletion was compatible with cell proliferation would identify situations where the DNA structures that are usually processed to lethal events by Rqh1 (in the absence of Top3) do not arise. This should help identify at which stage during recombination Rqh1 functions.

Rqh1 acts both downstream and upstream of the RecA homologue Rhp51. We find that *top3* loss of function does not cause inviability in *rhp51-d*, *rhp54-d*, *rhp55-d*, or *rad22-d* (*RAD52* homologue) backgrounds. Rhp51 is the *S. pombe* RecA homologue (39) and, by comparison with *E. coli* and *S. cerevisiae*, is assumed to form the nucleoprotein filaments required to initiate recombination (44). Rhp55 acts to mediate Rhp51 filament formation, and Rhp54 is thought to act later, after heteroduplex formation (44). The role of the *S. pombe* Rad52 homologue, Rad22, is ambiguous (41). It is probably involved in initiating and mediating Rhp51 filament formation. There are two straightforward explanations for the fact that, in all four of these mutants, Rqh1-dependent *top3-d* lethality is avoided: the first is that, in the processing of aberrant DNA structures arising spontaneously during DNA replication, Rqh1-Top3 acts after the formation of Rhp51 filaments. A second is that, in the absence of Top3, Rqh1 initiates a recombination event that is lethal. This could not occur when recombination is abolished.

In addition to using *top3-d* inviability as an assay, we have measured the survival of combinations of *rqh1*, *top3* and recombination mutants to UV-induced DNA damage. This provides evidence that Rqh1 and Top3 act after Rhp51 in DNA repair. Recombination mutants combined with either *top3-d* or *rqh1-d top3-d* did not show an increase in UV sensitivity, formally placing Rqh1-Top3 function within the recombination-dependent repair response (Fig. 4 and reference 42). Importantly, however, in the cases of *rhp51-d* and *rhp55-d* (in both cases recombination cannot occur due to the inability to form heteroduplex DNA), concomitant deletion of *rqh1*, *top3*, or both *rqh1* and *top3* resulted in a rescue of *rqh1-d top3-d* sensitivity at low doses of UV-induced DNA damage in both asynchronous and G_2-synchronized cells. (At higher doses, *rhp51-d* is more sensitive than *rqh1-d*, which may mask the effect.) This observation implies that, during the response to induced DNA damage, Rqh1-Top3 acts either downstream of Rhp51 (the same logic as given in hypothesis one above) or that Rqh1-Top3 acts before recombination (the same logic as given in hypothesis two).

Unlike what we found concerning response to intrinsic DNA damage (lethality), in the case of induced DNA damage, we were able to correlate the rescue data with observations based on cell biology: we find that Top3 foci are dependent on Rqh1 and that Rqh1 foci are partially dependent on both Rhp51 and Rhp18. Thus, the function of Rqh1 and Top3 is complicated, and we suggest that these data provide support for both hypotheses: i.e., that, if DNA damage is not processed by Rhp51 into recombination intermediates, it does not become an abortive substrate for Rqh1, which can act downstream. (Presumably, this damage can then be repaired by an alternative pathway, accounting for the rescue of *rqh1-d* sensitivity by concomitant *rhp51* or *rhp55* deletion.) In addition, based on epistasis analysis and the induction of foci, Rqh1 can act before Rhp51 (hypothesis two) in the Rhp18 UV response to DNA damage in G2 cells.

Because Rqh1 appears to act both upstream and downstream of recombination, depending on the DNA damage response pathway where it is functioning, we cannot precisely define a single linear pathway and thus suggest the model presented in Fig. 6 to account for these data. Furthermore, we cannot use the kinetics and dependency of focus formation to distinguish between the two hypotheses (upstream or downstream) during the processing of spontaneous lesions. However, we strongly favor a similar order of events. To extrapolate from the analysis of induced DNA damage, if the Rqh1-dependent *top3-d* lethality occurs downstream of recombination, in *top3-d* cells the Rqh1 helicase would act on recombination intermediates in such a way that cells entered mitosis with unresolved recombination structures. Thus, removing the helicase or recombination would suppress the lethality. Alternatively, the lethality of *top3-d* cells could be due to inappropriate processing by recombination proteins of DNA structures arising from Rhp18-mediated damage tolerance. This recombination event would then require Rqh1-Top3 for resolution and so would be lethal. In either case then, it would be the events downstream of recombination that are important for viability. This is supported by the fact that deletion of *rhp18*, although significantly reducing Rqh1 foci in response to UV damage, does not suppress the lethality of *top3-d* (Table 1).

A role for Rqh1 and Top3 during recombination repair in G_2. It has been established in several systems that eukaryotic RecA homologues form foci following DNA damage (23, 32, 47). However, RecA homologues are found at replication sites during the unperturbed S phase along with (in some instances) RecQ homologues (46, 51). Because recombination proteins and RecQ family helicases are involved in DNA metabolism during replication, it is important to establish if foci visualized following UV-induced DNA damage represent persisting replication forks or if they arise de novo as part of the DNA damage response. Consistent with data from other organisms, Rhp51 formed clear de novo foci when G_2 cells were irradiated with UV. In *S. pombe*, this correlated to the activity of the *uve1*-dependent repair pathway that is known to require recombination functions to repair UV-induced lesions.

In somewhat of a surprise to us, we observed that both Rqh1 and Top3 also formed de novo foci in a significant proportion of UV-damaged G_2 cells. Rqh1 clearly acts in multiple aspects of DNA metabolism. It is required during processing of DNA structures arising spontaneously, most probably within S phase, as evidenced by the increased spontaneous recombination observed in the null mutant (17). Rqh1 is also required for damage tolerance when DNA damage is encountered by the replication fork (42). This most probably reflects an involvement in several recombination-based mechanisms used to bypass DNA damage. The observation that loss of *rqh1* increases induced recombination following UV treatment probably reflects this function. Our observations that Rqh1 and Top3 form de novo foci provides evidence that Rqh1 also functions in the response to UV-induced DNA damage in G_2 cells. Several reports in the literature are consistent with RecQ family proteins acting in DNA repair outside S phase: Wu et al. (51) reported a physical interaction between BLM and RAD51 in humans and Sgs1 and Rad51 in *S. cerevisiae* and colocalization of BLM and RAD51 following DNA damage. Bischof et al. (5) also observed BLM focus formation after DNA damage, in this case in late S-G_2 cells. Caspari et al. (9) recently demonstrated that IR-induced DSBs in G_2 cells resulted in the formation of Rqh1 and Top3 foci and presented genetic evidence that suggests a function for Top3 in resolving Holliday junctions (reviewed in reference 7). Our data, which correlate with both clonogenic survival analysis of G_2 cells and the appearance of Rqh1 and Top3 foci in an Rhp51- and Rhp18-dependent manner, provide the direct evidence for a function of a RecQ helicase family member outside DNA replication and the first evidence that Rqh1-Top3 functions in G_2 in response to UV-induced DNA damage.

Top3 may act independently of Rqh1. It is intriguing to know if Rqh1 always acts in association with Top3. Certainly, it appears that Top3 is required to resolve RecQ family helicase-generated DNA structures in many systems, but it is not possible to ascertain directly if Rqh1 has roles in which it acts independently of Top3. Interestingly, although *rqh1-d* mutant cells were extremely slow growing when combined with *rad22-d*, a triple mutant of *rad22-d rqh1-d top3-d* was significantly more viable (see Fig. 4b, panel i, and Table 1). This suggests that, in this case, increased lethality is due to inappropriate Top3 activity. In other words, the rescue of the growth defect of *rqh1-d rad22-d* by deletion of *top3* is evidence that Top3 functions independently of Rqh1 but not that Rqh1 functions independently of Top3. This is consistent with work by Onodera et al. (43), who reported a functional and physical interaction between Sgs1 and Top3 and an Sgs1-independent function of Top3 in DNA recombination repair (43). In all our experiments we have not been able to separate Rqh1 function from Top3 function. Biochemical analysis showed that not all Top3 was coprecipitated with Rqh1. However, we also find that the majority of Rqh1 is insoluble and that the small percentage of soluble Rqh1 in an asynchronous cell extract most likely arises from the M-G_1 cells (data not shown). This precludes a thorough biochemical analysis by protein association.

Summary. Our data provide strong evidence that, where Rqh1 functions in a recombination-based pathway, it functions after Rhp51 filament formation. This would be consistent with models that predict that RecQ helicases help determine the correct substrate for appropriate strand invasion by reversing inappropriate heteroduplex intermediates. The fact that we also find evidence for Rqh1 acting before recombination proteins in certain circumstances may ultimately help to reconcile the differences in interpretation between work in *S. pombe* and models based on observations from *S. cerevisiae* that have suggested that RecQ helicases act before Rad51 (11).

ACKNOWLEDGMENTS

We acknowledge Thomas Caspari for advice and technical suggestions and sharing unpublished data.

This work was supported by CRC Grant SP2396/0201 (J.M.M.) and Danish Cancer Society Grant DP 00 093, the Danish Medical and Natural Science Research Councils, and the Novo Nordic Foundation (A.H.A.).

REFERENCES

1. **Bahler, J., J. Q. Wu, M. S. Longtine, N. G. Shah, A. McKenzie, A. B. Steever, A. Wach, P. Philippsen, and J. R. Pringle.** 1998. Heterologous modules for efficient and versatile PCR-based gene targeting in *Schizosaccharomyces pombe*. Yeast **14:**943–951.
2. **Barbet, N. C., and A. M. Carr.** 1993. Fission yeast wee1 protein kinase is not required for DNA damage-dependent mitotic arrest. Nature **364:**824–827.
3. **Bennett, R., M. Noirot-Gros, and J. Wang.** 2000. Interaction between yeast sgs1 helicase and DNA topoisomerase III. J. Biol. Chem. **275:**26898–26905.
4. **Bennett, R., J. Sharp, and J. Wang.** 1998. Purification and characterization of the Sgs1 DNA helicase activity of Saccharomyces cerevisiae. J. Biol. Chem. **273:**9644–9650.
5. **Bischof, O., S.-H. Kim, J. Irving, S. Beresten, N. A. Ellis, and J. Campisi.** 2001. Regulation and localization of the Bloom syndrome protein in response to DNA damage. J. Cell Biol. **153:**367–380.
6. **Broomfield, S., T. Hryciw, and W. Xiao.** 2001. DNA postreplication repair and mutagenesis in Saccharomyces cerevisiae. Mutat. Res. **486:**167–184.
7. **Carr, A. M.** 2002. DNA structure dependent checkpoints as regulators of DNA repair. DNA Repair **1:**983–994.
8. **Caspari, T., M. Dahlen, G. Kanter-Smoler, H. D. Lindsay, K. Hofmann, K. Papadimitriou, P. Sunnerhagen, and A. M. Carr.** 2000. Characterization of *Schizosaccharomyces pombe* Hus1: a PCNA-related protein that associates with Rad1 and Rad9. Mol. Cell. Biol. **20:**1254–1262.
9. **Caspari, T., J. M. Murray, and A. M. Carr.** 2002. Cdc2-cyclin B kinase activity links Crb2 and Rqh1-topoisomerase III. Genes Dev. **16:**1195–1208.
10. **Chakraverty, R. K., and I. D. Hickson.** 1999. Defending genome integrity during DNA replication: a proposed role for RecQ family helicases. Bioessays **21:**286–294.
11. **Chakraverty, R. K., J. M. Kearsey, T. J. Oakley, M. Grenon, M. A. de La Torre Ruiz, N. F. Lowndes, and I. D. Hickson.** 2001. Topoisomerase III acts upstream of Rad53p in the S-phase DNA damage checkpoint. Mol. Cell. Biol. **21:**7150–7162.
12. **Christensen, P. U., N. J. Bentley, R. G. Martinho, O. Nielsen, and A. M. Carr.** 2000. Mik1 levels accumulate in S phase and may mediate an intrinsic link between S phase and mitosis. Proc. Natl. Acad. Sci. USA **97:**2579–2584.
13. **Courcelle, J., and P. Hanawalt.** 1999. RecQ and RecJ process blocked replication forks prior to the resumption of replication in UV-irradiated Escherichia coli. Mol. Gen. Genet. **262:**543–551.
14. **Cox, M. M.** 2001. Historical overview: searching for replication help in all of the rec places. Proc. Natl. Acad. Sci. USA **98:**8173–8180.
15. **Craven, R. A., D. J. F. Griffiths, K. S. Sheldrick, R. E. Randall, I. M. Hagan, and A. M. Carr.** 1998. Vectors for the expression of tagged proteins in *Schizosaccharomyces pombe*. Gene **221:**59–68.
16. **DiGate, R. J., and K. J. Marians.** 1992. Escherichia coli topoisomerase III-catalyzed cleavage of RNA. J. Biol. Chem. **267:**20532–20535.
17. **Doe, C. L., J. Dixon, F. Osman, and M. C. Whitby.** 2000. Partial suppression of the fission yeast *rqh1*(-) phenotype by expression of a bacterial Holliday junction resolvase. EMBO J. **19:**2751–2762.
18. **Edwards, R. J., and A. M. Carr.** 1997. Analysis of radiation-sensitive mutants of fission yeast. Methods Enzymol. **283:**471–494.
19. **Fricke, W., V. Kaliraman, and S. Brill.** 2001. Mapping the DNA topoisomerase III binding domain of the Sgs1 DNA helicase. J. Biol. Chem. **276:**8848–8855.
20. **Gangloff, S., J. P. McDonald, C. Bendixen, L. Arthur, and R. Rothstein.** 1994. The yeast type I topoisomerase Top3 interacts with Sgs1, a DNA helicase homolog: a potential eukaryotic reverse gyrase. Mol. Cell. Biol. **14:**8391–8398.
21. **German, J., R. Archibald, and D. Bloom.** 1965. Chromosomal breakage in a rare and probably genetically determined syndrome of man. Science **148:**506–507.
22. **Goodwin, A., S.-W. Wang, T. Toda, C. Norbury, and I. D. Hickson.** 1999.

Topoisomerase III is essential for accurate nuclear division in *Schizosaccharomyces pombe.* Nucleic Acids Res. **27:**4050–4058.
23. **Haaf, T., E. I. Golub, G. Reddy, C. M. Radding, and D. C. Ward.** 1995. Nuclear foci of mammalian Rad51 recombination protein in somatic cells after DNA damage and its localization in synaptonemal complexes. Proc. Natl. Acad. Sci. USA **92:**2298–2302.
24. **Harmon, F., and S. Kowalczykowski.** 1998. RecQ helicase, in concert with RecA and SSB proteins, initiates and disrupts DNA recombination. Genes Dev. **12:**1134–1144.
25. **Harmon, F. G., R. J. DiGate, and S. C. Kowalczykowski.** 1999. RecQ helicase and topoisomerase III comprise a novel DNA strand passage function: a conserved mechanism for control of DNA recombination. Mol. Cell **3:**611–620.
26. **Johnson, F. B., D. B. Lombard, N. F. Neff, M. A. Mastrangelo, W. Dewolf, N. A. Ellis, R. A. Marciniak, Y. Yin, R. Jaenisch, and L. Guarente.** 2000. Association of the Bloom syndrome protein with topoisomerase IIIalpha in somatic and meiotic cells. Cancer Res. **60:**1162–1167.
27. **Kaliraman, V., J. R. Mullen, W. M. Fricke, S. A. Bastin-Shanower, and S. J. Brill.** 2001. Functional overlap between Sgs1-Top3 and the Mms4-Mus81 endonuclease. Genes Dev. **15:**2730–3740.
28. **Karow, J., R. Chakraverty, and I. Hickson.** 1997. The Bloom's syndrome gene product is a 3′-5′ DNA helicase. J. Biol. Chem. **272:**30611–30614.
29. **Karow, J., R. Newman, P. Freemont, and I. Hickson.** 1999. Oligomeric ring structure of the Bloom's syndrome helicase. Curr. Biol. **9:**597–600.
30. **Kaur, B., A. M. Avery, and P. W. Doetsch.** 1998. Expression, purification, and characterization of ultraviolet DNA endonuclease from Schizosaccharomyces pombe. Biochemistry **37:**11599–11604.
31. **Kitao, S., N. M. Lindor, M. Shiratori, Y. Furuichi, and A. Shimamoto.** 1999. Rothmund-Thomson syndrome responsible gene, *RECQL4*: genomic structure and products. Genomics **61:**268–276.
32. **Liu, Y., and N. Maizels.** 2000. Coordinated response of mammalian Rad51 and Rad52 to DNA damage. EMBO Rep. **1:**85–90.
33. **Maftahi, M., C. S. Han, L. D. Langston, J. C. Hope, N. Zigouras, and G. A. Freyer.** 1999. The *top3(+)* gene is essential in *Schizosaccharomyces pombe* and the lethality associated with its loss is caused by Rad12 helicase activity. Nucleic Acids Res. **27:**4715–4724.
34. **Marians, K. J.** 2000. Replication and recombination intersect. Curr. Opin. Genet. Dev. **10:**151–156.
35. **McCready, S. J., F. Osman, and A. Yasui.** 2000. Repair of UV damage in the fission yeast *Schizosaccharomyces pombe*. Mutat. Res. **451:**197–210.
36. **Michel, B., M.-J. Flores, E. Viguera, G. Grompone, M. Seigneur, and V. Bidnenko.** 2001. Rescue of arrested replication forks by homologous recombination. Proc. Natl. Acad. Sci. USA **98:**8181–8188.
37. **Mohaghegh, P., and I. D. Hickson.** 2001. DNA helicase deficiencies associated with cancer predisposition and premature aging disorders. Hum. Mol. Genet. **10:**741–746.
38. **Moreno, S., A. Klar, and P. Nurse.** 1991. Molecular genetic analysis of fission yeast *Schizosaccharomyces pombe*. Methods Enzymol. **194:**795–826.
39. **Muris, D. F. R., K. Vreeden, A. M. Carr, B. C. Broughton, A. R. Lehmann, P. H. M. Lohman, and A. Pastink.** 1993. Cloning the *RAD51* homologue of *Schizosaccharomyces pombe*. Nucleic Acids Res. **21:**4586–4591.
40. **Muris, D. F. R., K. Vreeken, A. M. Carr, C. Smidt, P. H. M. Lohman, and A. Pastink.** 1996. Isolation of the *Schizosaccharomyces pombe RAD54* homolog, *rhp54*$^+$, a gene involved in the repair of radiation damage and replication fidelity. J. Cell Sci. **109:**73–81.
41. **Muris, D. F. R., K. Vreeken, H. Schmidt, K. Ostermann, B. Clever, P. H. M. Lohman, and A. Pastink.** 1996. Homologous recombination in the fission yeast *Schizosaccharomyces pombe*: different requirements for the *rhp51*$^+$, *rhp54*$^+$ and *rad22*$^+$ genes. Curr. Genet. **31:**248–254.
42. **Murray, J. M., H. D. Lindsay, C. A. Munday, and A. M. Carr.** 1997. Role of *Schizosaccharomyces pombe* RecQ homolog, recombination, and checkpoint genes in UV damage tolerance. Mol. Cell. Biol. **17:**6868–6875.
43. **Onodera, R., M. Seki, A. Ui, Y. Satoh, A. Miyajima, F. Onoda, and T. Enomoto.** 2002. Functional and physical interaction between Sgs1 and Top3 and Sgs1-independent function of Top3 in DNA recombination repair. Genes Genet. Syst. **77:**11–21.
44. **Paques, F., and J. E. Haber.** 1999. Multiple pathways of double-strand-break-induced recombination in *Saccharomyces cerevisiae*. Microbiol. Mol. Biol. Rev. **63:**349–404.
45. **Stewart, E., C. R. Chapman, F. Al-Khodairy, A. M. Carr, and T. Enoch.** 1997. *rhq1*$^+$, a fission yeast gene related to the Bloom's and Werner's syndrome genes, is required for reversible S phase arrest. EMBO J. **16:**2682–2692.
46. **Tashiro, S., N. Kotomura, A. Shinohara, K. Tanaka, K. Ueda, and N. Kamada.** 1996. S phase specific formation of the human Rad51 protein nuclear foci in lymphocytes. Oncogene **12:**2165–2170.
47. **Tashiro, S., J. Walter, A. Shinohara, N. Kamada, and T. Cremer.** 2000. Rad51 accumulation at sites of DNA damage and in postreplicative chromatin. J. Cell Biol. **150:**283–291.
48. **Verkade, H., T. Teli, L. Laursen, J. Murray, and M. O'Connell.** 2001. A homologue of the Rad18 postreplication repair gene is required for DNA damage responses throughout the fission yeast cell cycle. Mol. Genet. Genomics **265:**993–1003.
49. **Watt, P. M., E. J. Louis, R. H. Borts, and I. D. Hickson.** 1995. Sgs1: a eukaryotic homolog of *E. coli* RecQ that interacts with topoisomerase II *in vivo* and is required for faithful chromosome segregation. Cell **81:**253–260.
50. **Wu, L., S. Davies, P. North, H. Goulaouic, J. Riou, H. Turley, K. Gatter, and I. Hickson.** 2000. The Bloom's syndrome gene product interacts with topoisomerase III. J. Biol. Chem. **275:**9636–9644.
51. **Wu, L., S. L. Davies, N. C. Levitt, and I. D. Hickson.** 2001. Potential role for the BLM helicase in recombinational repair via a conserved interaction with RAD51. J. Biol. Chem. **276:**19375–19381.
52. **Wu, L., and I. D. Hickson.** 2002. RecQ helicases and cellular responses to DNA damage. Mutat. Res. **509:**35–47.
53. **Yasui, A., and S. J. McCready.** 1998. Alternative repair pathways for UV-induced DNA damage. Bioessays **20:**291–297.
54. **Yonemasu, R., S. McCready, J. M. Murray, F. Osman, M. Takao, K. Yamamoto, A. R. Lehmann, and A. Yasui.** 1997. Characterization of the alternative excision repair pathway of UV-damaged DNA in *Schizosaccharomyces pombe*. Nucleic Acids Res. **25:**1553–1558.
55. **Yu, C.-E., J. Oshima, Y.-H. Fu, E. M. Wijsman, F. Hisama, R. Alisch, S. Matthews, J. Nakura, T. Miki, S. Ouasi, G. M. Martin, J. Mulligan, and G. D. Schellenberg.** 1996. Positional cloning of the Werner's syndrome gene. Science **272:**258–262.